The Canadian Mineralogist
Vol. 42, pp. 1275-1282 (2004)

IN SITU MEASUREMENTS OF THE H_2O:CO_2 RATIO IN FLUID INCLUSIONS BY INFRARED SPECTROSCOPY

ROBERT L. LINNEN[§]

Department of Earth Sciences, University of Waterloo, Waterloo, Ontario N2L 3G1, Canada

HANS KEPPLER

Mineralogisches Institut, Universität Tübingen, Wilhelmstr. 56, D-72074 Tübingen, Germany and Bayerisches Geoinstitut, Universität Bayreuth, D-95440 Bayreuth, Germany

S. MICHAEL STERNER

Fluid Inclusion Technologies Inc., 2217 North Yellowood Avenue, Broken Arrow, Oklahoma 74012, U.S.A.

ABSTRACT

Synthetic H_2O–CO_2 inclusions of variable molar volume and composition were analyzed above their homogenization temperature at 300°C by Fourier transform infrared spectroscopy. The ratio of the integrated absorbance of the antisymmetric stretching band of CO_2 near 2250 cm^{-1} and of the O–H stretching vibrations of H_2O around 3700 cm^{-1} varies systematically with composition, whereas the effect of bulk-fluid molar volume on this ratio appears to be small. The following empirical equation reproduces the observed relationship between the ratio of integrated absorbances A of H_2O over CO_2 and the molar H_2O/CO_2 ratio: $(H_2O/CO_2)_{molar} = 0.6978*(A_{H2O}/A_{CO2})^{1.378}$. This relationship can be applied to fluid inclusions with molar volumes between 30 and 50 cm^3/mole and for binary H_2O–CO_2 fluid mixtures. It should be used with caution beyond the conditions stated.

Keywords: fluid inclusion, infrared spectroscopy, analytical technique, high temperature, *in situ* measurement.

SOMMAIRE

Nous avons utilisé la spectroscopie infrarouge avec transformation de Fourier pour analyser des inclusions synthétiques d'une phase fluide H_2O–CO_2 (dont le volume molaire et la composition varient), à une température supérieure à leur homogénéisation, 300°C. Le rapport de l'absorbance intégrée de la bande d'étirement antisymétrique du CO_2 près de 2250 cm^{-1} à celle des vibrations d'étirement O–H près de 3700 cm^{-1} varie systématiquement avec la composition, tandis que l'effet du volume molaire de l'inclusion semble assez faible. L'équation empirique suivante rend compte de la relation observée entre le rapport des absorbances intégrées A de H_2O à celles du CO_2 et le rapport molaire H_2O/CO_2: $(H_2O/CO_2)_{molar} = 0.6978*(A_{H2O}/A_{CO2})^{1.378}$. On peut appliquer cette relation aux inclusions fluides ayant un volume molaire entre 30 et 50 cm^3/mole et à celles contenant un mélange binaire H_2O–CO_2. Par contre, on devrait s'en servir avec circonspection au-delà des conditions spécifiées.

(Traduit par la Rédaction)

Mots-clés: inclusion fluide, spectroscopie infrarouge, technique analytique, température élevée, mesure *in situ*.

INTRODUCTION

A major problem in the analysis of aqueous-carbonic fluid inclusions is the determination of their bulk composition. Normally, the molar volumes of the aqueous and carbonic phases at room temperature, together with the volume percentage of each phase, are used to calculate these bulk parameters. Because fluid inclusions are three-dimensional objects, commonly with irregular shapes, large errors can be associated with estimates of volume proportions, resulting in incorrect compositions, molar volumes and isochore extrapolation. Parry (1986) recognized this limitation and developed an iterative method to better constrain the bulk composition of fluid inclusions using temperatures of total homogenization and estimates of molar volume based on the proportions

§ *E-mail address*: rlinnen@uwaterloo.ca

of phases at room temperature. Schwartz (1989) developed a graphical method to determine the bulk compostion and molar volume of fluid inclusions. However, for inclusions that homogenize at P–*X* conditions where the H_2O–CO_2 solvus is insensitive to temperature, neither of these methods can be used to accurately determine the composition of a fluid inclusion. For example, the H_2O–CO_2 solvus at 2000 bars is nearly flat for fluid compositions between from 15 and 75 mol.% CO_2 (Tödheide & Franck 1963, Sterner & Bodnar 1991). A non-destructive technique that can be used to determine the composition of individual inclusions would thus be highly valuable. Two such techniques are Raman spectroscopy and infrared spectroscopy. However, in order for these techniques to be useful in determining bulk composition, the analyses must be obtained at a temperature above the two-phase solvus, *i.e.,* above the total (aqueous-carbonic) homogenization temperature (the reasons for this are discussed in the section entitled Fourier Transform Infrared Spectrometer).

To date, only Raman spectra have been collected for H_2O–CO_2 fluid inclusions at P–T conditions above the two-phase solvus (Dubessy *et al.* 1999). Whereas this technique shows promise, it is not developed to the extent where Raman spectroscopy can be used to determine the H_2O:CO_2 ratio of a fluid in an inclusion. Fourier transform infrared (FTIR) spectroscopy of fluid inclusions has primarily been applied to the analysis of petroleum in fluid inclusions (*e.g.,* Pironon *et al.* 2001), but has also been shown to be useful in the analysis of aqueous-carbonic fluid inclusions (*e.g.,* Wopenka *et al.* 1990, Brown 1992). In this study, we present FTIR results for aqueous-carbonic inclusions with a variety of compositions and molar volumes, determined at P–T conditions in the one-phase field. We use these data to establish a calibration curve for the FTIR analysis of H_2O–CO_2 inclusions ranging in composition from 12.5 to 62.5 mol.% CO_2. In principle, the equation can be extended to the entire range of H_2O–CO_2 compositions.

Equipment and Method

Synthetic fluid inclusions

The fluid inclusions analyzed in this study were synthesized by Sterner & Bodnar (1991). The homogenization temperatures of the carbon dioxide portion of the inclusion, as well as temperatures of total (aqueous-carbonic) homogenization for all fluid inclusions were determined using a Fluid Inc.® heating–freezing stage, hereafter referred to as the "normal stage". These temperatures were determined before and after the high-temperature FTIR measurements and are the same, within the error limits given on Table 1, indicating that the inclusions did not stretch or leak. Most of these temperatures were previously determined by Sterner & Bodnar (1991), and the homogenization temperatures determined here are in excellent agreement with their findings.

An aqueous-carbonic fluid inclusion at P–T conditions below its temperature of total homogenization is a two-component system, and the compositions of the coexisting CO_2-rich and H_2O-rich phases both change as a function of temperature and pressure (defining a solvus). However, above the temperature of total homogenization, the inclusion can be described by one component (the bulk composition) and one phase, and thus the system (the fluid inclusion) has two degrees of freedom. Consequently, a single-phase inclusion at fixed temperature (*e.g.,* 300°C) has only one degree of freedom. If the molar volume is known (in this case from Sterner & Bodnar 1991), then the system is invariant. The fluid-inclusion data in this study are presented in terms of composition and molar volume and because each inclusion at 300°C is invariant.

Fourier transform infrared spectrometer

The synthetic H_2O–CO_2 fluid inclusions were analyzed on a Bruker IFS 120 HR spectrometer equipped with a Bruker IR microscope, Globar source, CaF_2 beam-splitter and a narrow-band MCT detector. The microscope operates under a continuous stream of dry air. To diminish interference from atmospheric CO_2 and H_2O, nitrogen was used as a carrier gas for the modified fluid-inclusion stage (see below), and a separate tube was used to flush a constant supply of N_2 at the surface of the sample chamber, below the microscope objective. The flow rate of the N_2 carrier gas in the heating experiments was constant at 30 SCFH (standard cubic feet per hour).

An adjustable rectangular aperture in the rear focal plane of a 15× Cassegranian objective (working distance 32 mm) was used to define the area probed by the infrared beam. The aperture was adjusted such that the spot size is somewhat smaller than the inclusion, which was greater than 8×10 μm for most of the inclusions in this study. Since we measured spectra in the near-infrared range between 2000 and 4000 cm^{-1}, where the wavelength of the infrared beam is in the range 3 to 5 μm, we are confident that no major diffraction-induced effects occurred on inclusions of this size. Reflection or refraction at the inclusion surface only changes the total amount of radiation reaching the detector. This will result in a shift of the baseline, but it does not affect the height of the absorption bands.

Because inclusions have an irregular shape and are heterogeneous (two or three phases are present at room temperature), the CO_2 mole fraction cannot be determined at room temperature. Quantitative analyses can only be made if the fluid analyzed is a single phase. The pressure of homogenization can be very high in many H_2O–CO_2 fluid inclusions (in excess of 2 kbar, *cf.* Sterner & Bodnar 1991). Thus the pressure during the

TABLE 1. MICROTHERMOMETRIC AND FTIR DATA ON SYNTHETIC H_2O–CO_2 FLUID INCLUSIONS

$X(CO_2)$	Molar volume cm^3/mol.	P kbar	T °C	T_h^1 °C	$T_h^1CO_2$ °C	T_h^2 °C	$T_h^2CO_2$ °C	H_2O/CO_2 peak area	No.	Std. dev.	Max. peak height
0.125	34.5	3	700	-	27.25_v	307_l (1.0)	26.5_v (0.3)	5.69[a]	8	0.69	1.2
0.125	31.5	4	700	289_l	29.7_v	291_l (0.5)	29.7_v (0.1)	4.58	11	0.47	0.23
0.25	31.8	4	700	282_l	28.5_l	286_l (1.0)	28.6_l (0.1)	2.59	3	0.13	0.14
0.25	30.2	4	600	275_l	27.8_v	278_l (0.5)	28.1_l (0.1)	2.99	2	0.01	0.2
0.25	28.2	4	500	270_l	22.6_l	271_l (1.0)	22.9_l (0.1)	2.99	4	0.22	0.2
0.25	25.4	2	600	306_{cr}	30.6_v	308_{cr} (0.1)	31.0_v (0.1)	3.14[b]	3	0.02	0.15
0.375	35.4	4	700	276_v	25.0_l	276_l (0.5)	25.1_l (0.1)	1.68	6	0.23	0.16
0.375	33.4	4	600	273_v	21.6_l	273_l (1.0)	21.6_l (0.1)	2.18	4	0.18	0.34
0.50	70.7	1	500	-	30.3_v	300_v (6.0)	30.4_v (0.1)	0.99	6	0.32	0.36
0.50	50.3	2	600	284_v	30.7_l	284_v (2.0)	30.7_l (0.1)	1.30	4	0.24	0.20
0.50	42.9	3	700	-	27.1_l	277_v (3.0)	27.0_l (0.2)	1.76	3	0.11	0.7
0.50	40.1	3	600	-	24.3_l	275_v (1.0)	25.8_l (0.1)	1.57	4	0.05	0.9
0.50	38.8	4	700	268_v	20.3_l	271_v (3.0)	20.4_l (0.2)	1.21	4	0.06	1.15
0.50	36.7	4	600	273_v	16.7_l	273_v (2.0)	16.7_l (0.2)	1.43	3	0.07	0.25
0.625	39.7	4	600	258_v	11.5_l	261_v (3.0)	11.6_l (0.3)	0.86	3	0.08	0.25

T_h^1 is the temperature of total (aqueous-carbonic) homogenization, $T_h^1CO_2$ is the temperature of CO_2 homogenization, taken from the study of Sterner & Bodnar (1991), for fluid inclusions with the compositions and molar volumes trapped at the given P–T conditions. The subscripts l, v and cr denote homogenization to the liquid, vapor or critical phase, respectively. T_h^2 and $T_h^2CO_2$ are the temperatures of homogenization for the same samples, as determined in this study. The errors (±°C) are given in brackets. The area ratio of the H_2O and CO_2 peaks were all determined from spectra obtained at 300°C, except for [a]analysis, at 320°C, and [b]analysis, at 315–320°C. No. is the number of measurements. The standard deviation (1σ) pertains to the area ratio of the H_2O and CO_2 peaks.

analysis should be as low as possible to prevent inclusions from decrepitating, *e.g.,* at temperatures near that of homogenization. Therefore, most of the inclusions in this study were analyzed at 300°C. In a few cases, the temperature of total homogenization was above 300°C, and in these cases, the inclusions were analyzed at a temperature approximately ten degrees above the temperature of homogenization (Table 1).

The spectra were collected with a resolution of 4 cm^{-1} and typically consist of 500 to 1000 scans (a few minutes of data collection). The background was measured with the beam passing through inclusion-free quartz in the same sample at 300°C. The baseline was defined by the parts of the spectra with wavenumbers less than 2240, between 2500 and 3100, and above 4150 cm^{-1}. The peak areas of H_2O and CO_2 were obtained by integrating the absorbances over the wavenumber ranges of 3100 to 4150 cm^{-1}, and 2240 to 2500 cm^{-1}, respectively, after baseline correction. Occasionally, the small size and irregular shape of the inclusions in this study did cause problems. In some cases, the spectra collected were of poor quality, either with a sloped background or a jog in the background at one side of a peak. These spectra were rejected.

Fluid-inclusion stages

The homogenization temperatures of the carbon dioxide, as well as temperatures of total (aqueous-carbonic) homogenization of all fluid inclusions, were determined using a Fluid Inc.® heating–freezing stage. The thermocouple was calibrated using the melting temperatures of CO_2 in a synthetic H_2O–CO_2 fluid inclusion, the melting temperature of H_2O in a pure H_2O inclusion, and the temperature of homogenization of a critical H_2O synthetic fluid inclusion. The accuracy of the homogenization temperatures of CO_2 (≤31°C) is better than ±0.1°C, and that of the temperatures of total homogenization (250–350°C) is approximately ±1.0°C.

A normal heating–freezing stage is not suitable to use in infrared spectroscopy because the glass or quartz plates in the sample chamber will absorb infrared radiation and decrease the signal-to-noise ratio. The presence of trace H_2O in the glass plates will also interfere with the determination of H_2O in the fluid inclusions. To avoid these problems, we removed the glass plates in the sample chamber of a USGS-type heating–freezing stage and replaced them with a single CaF_2 window (~1 mm thick) and a spacer ring (also ~1 mm thick) in both the upper and lower halves of the chamber (Fig. 1). The sample was held on an Inconel disk (~0.015 mm thick) that contains a triangular hole. This setup changes the thermal gradients of the stage, and consequently the new sample chamber must be recalibrated. The modified fluid-inclusion stage was calibrated using a synthetic critical H_2O fluid inclusion, as well as the homogenization temperatures of the synthetic H_2O–CO_2 inclusions, as determined in this study using the normal stage. The

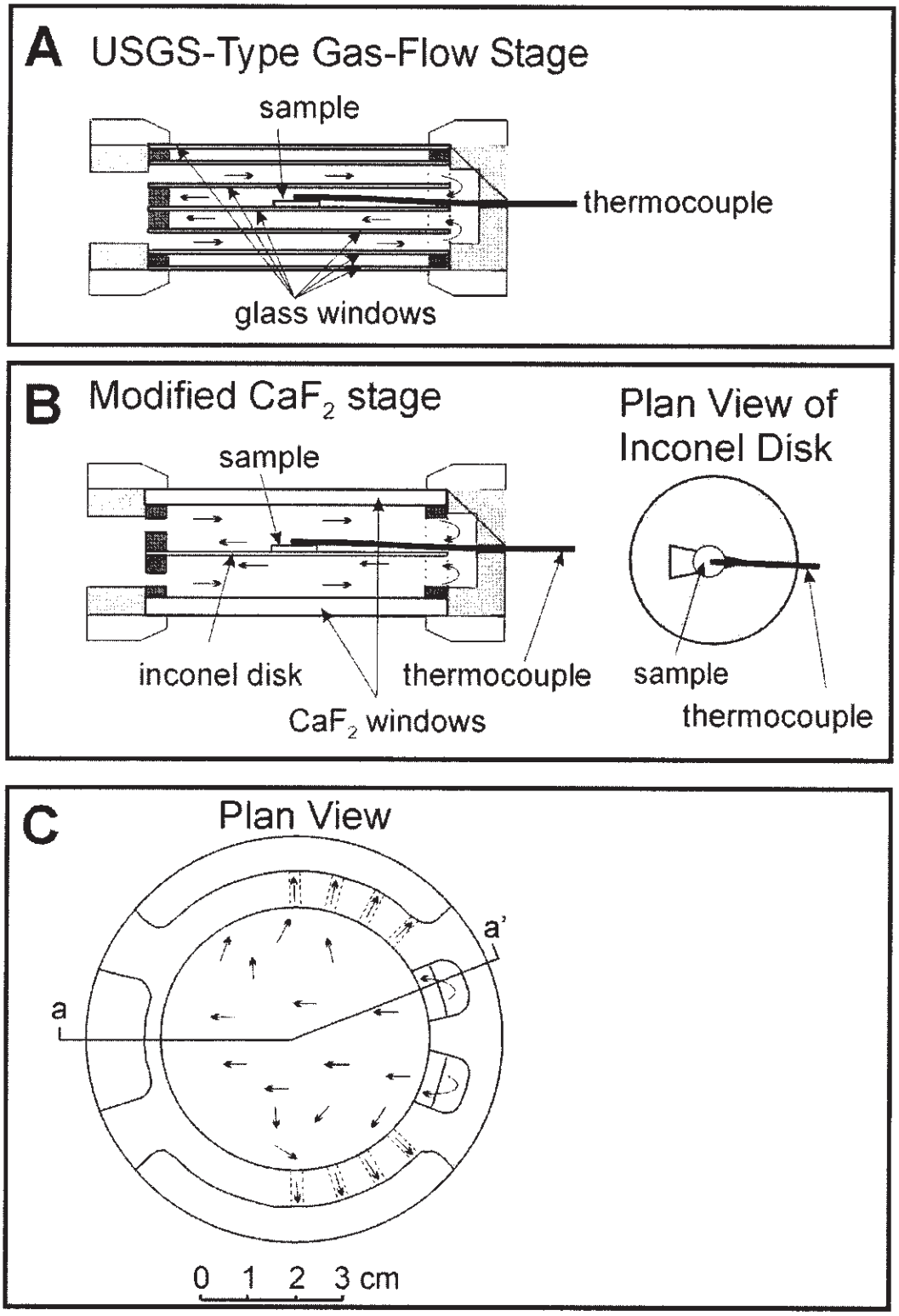
A
USGS-Type Gas-Flow Stage
sample
thermocouple
glass windows
B
Modified CaF_2 stage
sample
inconel disk
thermocouple
CaF_2 windows
Plan View of
Inconel Disk
sample
thermocouple
C
Plan View
a
a'
0 1 2 3 cm

thermal gradient (the difference between the temperature of homogenization and that of the thermocouple) in the modified stage was <2°C if the thermocouple tip is positioned <0.6 mm from the inclusion analyzed. Thus, the accuracy and the precision of temperature measurements with the CaF_2 setup are comparable to those with the normal gas-flow stage. The temperature of total homogenization, determined on the normal stage, also served as an internal standard for the modified stage. The difference in temperature between the normal and modified stages was better than ±5°C.

Results

In Figure 2, we show two spectra from the same fluid inclusion with a bulk composition of 12.5 CO_2 and a molar volume of 31.5 cm^3/mole. One spectrum was collected for the aqueous portion of the inclusion (~2.3 mol.% dissolved CO_2) at 22°C, and the other is from the one-phase field at 300°C (T_h = 289°C). There is an increase of the relative area of the CO_2 peak in the 300°C spectrum, and a corresponding decrease for that of H_2O, which indicates a higher CO_2 content in the fluid. There is also a peak shift to higher wavenumbers for H_2O at higher temperatures, related to a decrease in the strength of the hydrogen bond.

It is very difficult to assign an error to the analytical results because each inclusion has a unique size and shape. Consequently, each inclusion will have its own error (*cf.* Wopenka *et al.* 1990). To get an idea of the reproducibility of the technique, a single fluid inclusion (12.5 mol.% CO_2 and a molar volume of 31.5 cm^3/mole) was analyzed on three different days, so that variables such as analysis area, gas flow-rate, *etc.* were all slightly different (Fig. 3). The ratio of the H_2O and CO_2 peak areas for these three analyses is 4.58 ± 0.47 (*i.e.,* the reproducibility is within approximately 10%).

Figure 4 shows spectra for inclusions with 12.5, 25, 37.5, 50 and 62.5 mol.% CO_2, scaled such that the height of the CO_2 peak for each inclusion is roughly equal. With increasing CO_2 content of the fluid inclusion, there is an antithetic decrease of the peak area of H_2O. Another factor that may affect the ratio of the H_2O:CO_2 peak areas of an inclusion is the molar volume of the fluid (the strength of the hydrogen bond is related to molar volume; see below). Spectra were obtained for several different molar volumes for most of the compositions investigated. The largest number of bulk molar volumes examined was for the 50 mol.% CO_2 composition, and the six spectra for molar volumes ranging from 36.7 to 70.7 cm^3/mole are shown in Figure 5. The CO_2 peaks in this figure are all scaled to approximately the same height. Visual inspection suggests that there is little variation in the ratio of the H_2O:CO_2 peak areas, except perhaps for the sample with the largest molar volume.

Figure 6 shows the variation in the peak-area ratios as a function of molar volume. There is a rather poor correlation between these two parameters. There may be a negative dependence of the peak-area ratio on molar

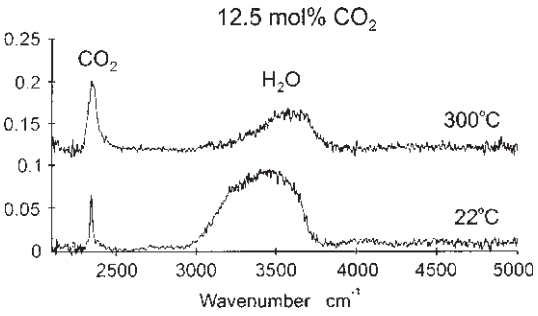

FIG. 2. Two spectra from the same fluid inclusion with a bulk composition of 12.5 mol.% CO_2 and molar volume of 31.5 cm^3/mole. The lower spectrum was collected for the aqueous portion (~2.3 mol.% dissolved CO_2) of the inclusion at 22°C, and the upper spectrum is from the one-phase field at 300°C (T_h = 289°C).

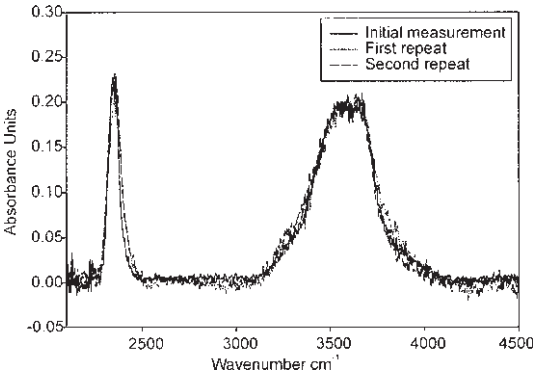

FIG. 3. Reproducibility of measurements. Three different spectra collected from the same fluid inclusion (12.5 mol.% CO_2 and molar volume of 31.5 cm^3/mole) are shown by three different symbols. The height of the CO_2 peak for the three spectra is scaled to approximately the same value. The area ratio of the H_2O and CO_2 peaks for these three spectra is 4.58 ± 0.47 (*i.e.,* the reproducibility is within approximately 10%).

FIG. 1. Fluid Inclusion Sample Chamber. A. A "normal" USGS-type sample chamber, drawn after the diagram in Roedder (1984). B. A sketch of the modified CaF_2 sample chamber used in this study. C. A plan view of either stage A or B, drawn after the diagram in Roedder (1984).

volume for the 50 mol.% CO_2 composition, but the data are scattered. There are not enough data-points for the 25 and 37.5 mol.% CO_2 compositions to definitively state whether or not the area ratio of H_2O and CO_2 peaks is dependent on molar volume.

In Figure 7, we summarize the data obtained in this study, and show the ratio of H_2O and CO_2 peak areas as a function of the molar H_2O:CO_2 ratio of the inclusion. Because of the possible dependence of peak-area ratio on molar volume, different symbols are used for bulk molar volumes of inclusions with 20–30, 30–40. and greater than 50 cm^3/mole. The ratio of the H_2O and CO_2 peak areas depends primarily on the molar H_2O:CO_2 ratio of the inclusion, and molar volume only exerts a secondary effect, if at all. The following empirical equation reproduces the observed relationship between the ratio of integrated absorbance A of H_2O over that of CO_2 and the molar H_2O:CO_2 ratio:

$$(H_2O/CO_2)_{molar} = 0.6978*(A_{H2O}/A_{CO2})^{1.378} \quad (1).$$

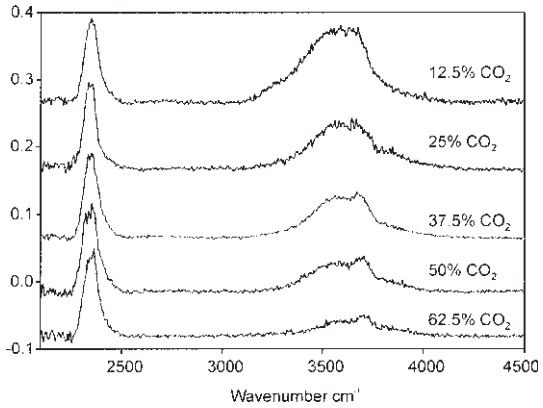

FIG. 4. The effect of varying composition on area ratio H_2O and CO_2 peaks.

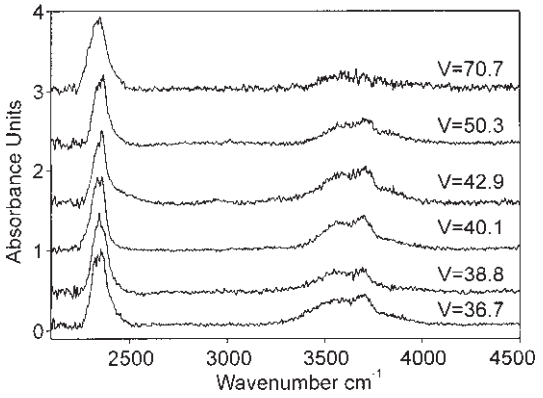

FIG. 5. The effect of varying molar volume on area ratios of H_2O and CO_2 peaks. All of the spectra are collected for inclusions with 50 mol.% CO_2, and the molar volumes (cm^3/mol.) are given on the right-hand side of the diagram.

DISCUSSION

Dependence of extinction coefficients on composition and molar volume

The infrared absorbance A is related to the concentration c of a species in a fluid and to the thickness d of the fluid layer by the Lambert Beer law:

$$A = \log I_0/I = \varepsilon\ c\ d \quad (2)$$

where I_0 is the intensity of the incident beam, I is the intensity of the beam after passing through the sample, ε is the extinction coefficient, c is the concentration of the species and d is the thickness of the sample. If the absorbances of two bands are compared, *e.g.,* the bands of H_2O and CO_2 measured on the same sample of fluid with identical thickness, it follows that:

$$A_{H2O}/A_{CO2} = \varepsilon_{H2O}\ c_{H2O} / \varepsilon_{CO2}\ c_{CO2} \quad (3)$$

This equation would imply that for constant extinction coefficients, A_{H2O}/A_{CO2} should be directly proportional to the molar ratio of H_2O and CO_2. Unfortunately, extinction coefficients are generally not constant; they vary with composition and molar volume of the fluid. In particular, the extinction coefficients for the infrared bands of H_2O are known to vary strongly with the strength of hydrogen bonding (*e.g.,* Franck 1974). The

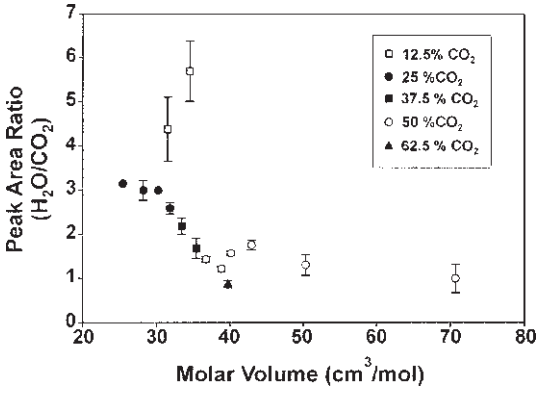

FIG. 6. Variation of the area ratio of H_2O and CO_2 peaks as a function of molar volume of the inclusion.

strength of hydrogen bonds decreases if the average distance between H_2O molecules in the fluids increases. This increase can result from a dilution by an inert component such as CO_2 or from an increase in molar volume, which directly increases the average distance between the molecules. Both effects will lead to a decrease in extinction coefficients. There is, however, no simple, theoretically sound mathematical formula that would account for this phenomenon. It is therefore not surprising that the data in Figure 7 deviate from a simple proportionality between peak-area ratio and molar ratio of H_2O and CO_2.

At high molar volume, hydrogen bonds become weaker, and the extinction coefficients, smaller (*e.g.,* Franck 1974), which implies reduced absorbances under otherwise identical conditions. This effect is probably seen in the uppermost spectrum in Figure 5 (V = 70.7), where the H_2O band appears to be anomalously weak. In general, however, the effect of molar volume on the area ratio of H_2O and CO_2 peaks found in this study is remarkably small. Two factors may contribute to this behavior. Firstly, the measurements were obtained at 300°C, where hydrogen bonding effects are much weaker than at room temperature. Secondly, the presence of CO_2 in the samples further reduces the strength of hydrogen bonds.

Potential sources of error in the analysis of fluid inclusions by FTIR

For quantitative analyses by infrared spectroscopy, the sample must be homogeneous in composition. Moreover, the infrared beam should pass through a layer of constant thickness, in this case a fluid layer of constant thickness. Whereas the first criterion is certainly fulfilled if the measurements are carried out at a temperature above the homogenization of the fluid inclusion, it is more diffcult to meet the second criterion. Fluid inclusions commonly have an irregular shape. Even if a small spot-size is used, different parts of the beam will pass through layers of slightly different thickness. This effect can cause substantial systematic errors, and even more serious errors may be encountered if some part of the beam does not pass through the sample at all, *e.g.*, if the aperture used is larger than the image of the fluid inclusion.

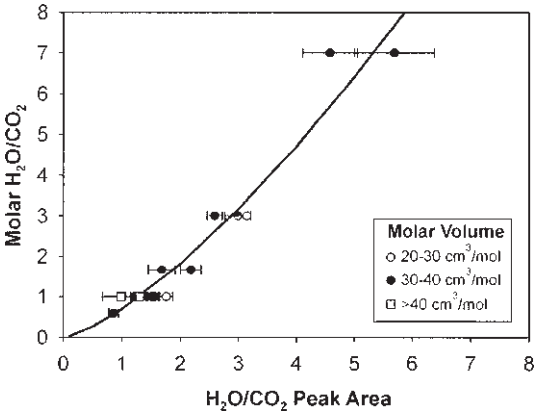

FIG. 7. Variation of the area ratio of the H_2O and CO_2 peaks as a function of the molar composition of the inclusion. The curve shown is a fit using the equation $(H_2O/CO_2)_{molar} = 0.6978*(A_{H2O}/A_{CO2})^{1.378}$, where $(H_2O/CO_2)_{molar}$ is the molar compositions and A_{H2O}/A_{CO2} is the peak-area ratio.

In order to illustrate the potential errors that may be encountered in the analysis of fluid inclusions by FTIR, we now consider a H_2O–CO_2 inclusion of constant, well-defined thickness, which yields absorbances of the CO_2 and H_2O bands of 2 and 1, respectively. According to the Lambert Beer law, only 1% of the incident radiation is transmitted in frequency range of the CO_2 band, whereas 10% of the incident radiation is transmitted in the frequency range of the H_2O band.

$$A_{CO2} = 2 = \log I_0/I \therefore I = 0.01\ I_0 \quad (4)$$

$$A_{H2O} = 1 = \log I_0/I \therefore I = 0.1\ I_0 \quad (5)$$

$$A_{CO2}/A_{H2O} = 2 \quad (6)$$

Now we assume that the same inclusion is measured with a beam area twice the size of the inclusion. In this case, 50% of the beam will not hit the inclusion and will reach the detector without reduction in intensity, whereas the other half of the beam will be partially absorbed by the sample. In this situation, the following absorbances will be observed:

$$A_{CO2} = \log I_0/I = \log [\ I_0 / (0.5\ I_0 + 0.5 \pm 0.01\ I_0)] = \log 1.98 = 0.30 \quad (7)$$

$$A_{H2O} = \log I_0/I = \log [\ I_0 / (0.5\ I_0 + 0.5 \pm 0.1\ I_0)] = \log 1.82 = 0.26 \quad (8)$$

$$A_{CO2}/A_{H2O} = 1.14 \quad (9)$$

This model calculation shows that FTIR analyses will not yield meaningful values of the ratio if some part of the beam does not pass through the sample. Such a geometry of measurement will always have two consequences: 1) the absolute measured absorbances are far too low, and 2) the ratio of absorbances of the two bands is closer to unity than in reality. In principle, the same, albeit smaller, effect is to be expected if the thickness of the sample is not uniform.

The model calculation outlined above illustrates an extreme case, since the absorbances of the sample are very high and therefore the measured intensity of the beam is strongly affected if even a small fraction of the

beam does not pass through the sample. In general, the potential error observed under these conditions will decrease if the sample absorbs only weakly.

If a sample has a well-defined thickness, *e.g.,* if the upper and the lower surface of the part of the inclusion analyzed are virtually parallel to each other, absorbances can be measured to ±0.01 units of linear absorbance. A slight curvature of the inclusion surface will not affect the measurement, since the beam used in commercial spectrometers is itself slightly divergent. Serious errors are, however, to be expected if the part of the inclusion measured has a very irregular shape, if the inclusion is smaller than the beam diameter, or if the inclusion is very thick, resulting in absorbances above 1, which cannot be measured accurately.

Comparison of Raman and FTIR spectroscopy as tools for the analysis of fluid inclusions

Infrared and Raman spectroscopy have distinct advantages and disadvantages in the quantitative analysis of fluid inclusions. With Raman spectroscopy, one measures light scattering induced by a laser beam, which usually operates in the visible range of frequencies. Owing to the small wavelength of incident and scattered radiation (about 1 μm), very small inclusions can be measured. Although it is generally easy to obtain Raman spectra of fluid inclusions for qualitative analyses, any quantification is difficult. Measurement of absolute intensities of scattering is virtually impossible. Even relative intensities of two bands depend, however, on instrumental parameters, such as the aperture of the objective used or the quantum yield of the detector, which changes with frequency and will be different from detector to detector. For this reason, a calibration of relative intensities of the Raman spectra as a function of the composition of a sample will invariably depend on instrumental parameters and cannot be directly transferred from one laboratory to another.

Infrared spectroscopy requires somewhat larger inclusions than Raman spectroscopy, since the wavelength of the infrared beam used is on the order of 3 to 5 μm, and any inclusion below these dimensions would cause diffraction of the beam. On the other hand, infrared absorbance can be measured in absolute terms, and the data obtained on the same sample will generally be reproducible within 1%, even if different spectrometers in different laboratories are used for the measurements. Our calibration therefore allows the quantitative analysis of H_2O–CO_2 inclusions over a considerable range of densities, ranging in composition from 12.5 to 62.5 mol.% CO_2. In principle, the equation can be extended to the entire range of H_2O–CO_2 compositions. If inclusions of very irregular shape are avoided, the accuracy of these measurements should be on the order of a few percent of molar composition.

Acknowledgements

This work was conducted at the Bayerisches Geoinstitut (BGI) at Bayreuth, Germany. All three authors gratefully acknowledge BGI for the financial support provided for this work. We also thank H. Schulze of BGI for the preparation of the doubly polished sections. The manuscript was improved by reviews from Bob Bodnar and Penny King, as well as the editorial comments of Dan Kontak and Bob Martin.

References

Brown, P.E. (1992): Micro-infrared spectroscopic analysis of fluid inclusions and minerals. *Goldschmidt Conf., Program Abstr.*, A14.

Dubessy, J., Moissette, A., Bakker, R.J., Frantz, J.D. & Zhang, Y.G. (1999): High-temperature Raman spectroscopic study of H_2O–CO_2–CH_4 mixtures in synthetic fluid inclusions: first insights on molecular interactions and analytical implications. *Eur. J. Mineral.* **11**, 23-32.

Franck, E.U. (1974): Polar and ionic fluids at high pressures and temperatures. *Pure and Applied Chem.* **38**, 449-468.

Parry, W.T. (1986): Estimation of X_{CO2}, P, and fluid inclusion volume from fluid inclusion temperature measurements in the system NaCl–CO_2–H_2O. *Econ. Geol.* **81**, 1009-1013.

Pironon, J., Thiery, R., Ayt Ougougdal, M., Teinturier, S., Beaudoin, G. & Walgenwitz, F. (2001): FT-IR measurements of petroleum fluid inclusions: methane, *n*-alkanes and carbon dioxide quantitative analysis. *Geofluids* **1**, 2-10.

Roedder, E. (1984): Fluid inclusions. *Rev. Mineral.* **12**.

Schwartz, M.O. (1989): Determining phase volumes of mixed CO_2–H_2O inclusions using microthermometric measurements. *Mineral. Deposita* **24**, 43-47.

Sterner, S.M. & Bodnar, R.J. (1991): Synthetic fluid inclusions. X. Experimental determination of P–V–T–X properties in the CO_2–H_2O system to 6 kb and 700°C. *Am. J. Sci.* **291**, 1-54.

Tödheide, K. & Franck, E.U. (1963): Das Zweiphasengebeit und die kritische Kurve im Kohlendioxid–Wasser bis zu Drucken von 3500 bar. *Z. Phys. Chem.* N.F. **37**, 387-401.

Wopenka, B., Pasteris, J.D. & Freeman, J.J. (1990): Analysis of individual fluid inclusions by Fourier transform infrared and Raman microspectroscopy. *Geochim. Cosmochim. Acta* **54**, 519-533.

Received April 19, 2003, revised manuscript accepted September 6, 2003.